Supramolecular Chemistry
Publication details, including instructions for authors and subscription information:
http://www.informaworld.com/smpp/title~content=t713649759

Colorimetric anion sensing by polyamide models containing urea-binding sites

Noelia San-José[a]; Ana Gómez-Valdemoro[a]; Saturnino Ibeas[a]; Félix Clemente García[a]; Felipe Serna[a]; José Miguel García[a]
[a] Departamento de Química, Facultad de Ciencias, Universidad de Burgos, Burgos, Spain

Online publication date: 05 May 2010

To cite this Article San-José, Noelia , Gómez-Valdemoro, Ana , Ibeas, Saturnino , García, Félix Clemente , Serna, Felipe and García, José Miguel(2010) 'Colorimetric anion sensing by polyamide models containing urea-binding sites', Supramolecular Chemistry, 22: 6, 325 — 338
To link to this Article: DOI: 10.1080/10610270903531549
URL: http://dx.doi.org/10.1080/10610270903531549

Supramolecular Chemistry
Vol. 22, No. 6, June 2010, 325–338

Taylor & Francis
Taylor & Francis Group

Colorimetric anion sensing by polyamide models containing urea-binding sites

Noelia San-José, Ana Gómez-Valdemoro, Saturnino Ibeas, Félix Clemente García, Felipe Serna and José Miguel García*

Departamento de Química, Facultad de Ciencias, Universidad de Burgos, Plaza de Misael Bañuelos s/n, E-09001 Burgos, Spain

(*Received 10 September 2009; final version received 2 December 2009*)

Novel colorimetric polyamide model compounds for anion-sensing applications are described. Light beige solutions of one of the models (**M3**) in DMSO develop a red to yellow-reddish colour upon addition of some anions, including OH^-, F^-, HCO_3^-, PO_4^{3-}, AcO^-, benzoate$^-$, oxalate^{2-} and *p*-toluenesulphonate$^-$. In contrast, they remain unchanged in the presence of $CH_2ClCO_2^-$, $H_2PO_4^-$, CF_3CO^{2-}, Br^-, methanesulphonate$^-$, Cl^- or I^-. The reddish colour caused by the addition of basic anions is due to the deprotonation of the urea groups, while the yellowish colour corresponds to the modification of the electron density surrounding the urea group due to complexation. The development of the yellow colour of DMSO solutions of **M3** upon addition of acetate ions and the disappearance of the red colour of solutions of **M3**/fluoride by the displacement of acetate ions can serve as a novel colorimetric assay for the titration of the acetate anion, with detection limits close to 1 ppb. The host:guest stoichiometry (polyamide model compound:anion complexes) and the stability constants of complexes were determined by ^{1}H NMR.

Keywords: urea-binding sites; anion sensing; polyamide model compounds

1. Introduction

The development of selective and sensitive materials for the colorimetric detection of anionic, cationic and neutral molecules is a topic of current scientific interest (*1–7*). In particular, the sensing of anions has drawn considerable attention because charged chemical species are ubiquitous and play major roles in many chemical and biological processes. Detection is often based on the design and synthesis of receptors (host molecules) capable of selectively binding anionic species (guest molecules) with a concomitant change in a measurable macroscopic property, such as fluorescence or UV–vis spectra. The field of synthetic anion receptor chemistry is one of the fastest growing disciplines within supramolecular chemistry.

Methodologies based on colorimetric changes of host–guest interactions are especially attractive for their potential use in naked-eye screening applications, especially in situations where conventional techniques are not appropriate or are expensive, or in the development of screening applications that can be used by non-scientist personnel.

The design and syntheses of molecules with selective anionic receptor sites are complex, due mainly to the variety of geometric shapes of anions. The recognition of anions in aqueous environments by biological systems is achieved via hydrogen bonding by highly organised proteins with partially hydrophobic and sterically well-defined complexation sites in the interior of the protein. The protein behaves as a hydrophilic macromolecule, surrounded by water, with partially hydrophobic binding sites where hydrogen bonds, or other feeble interactions, between these sites and the substrates can be formed in the absence of competition with water (*8–12*).

The complexation properties of such receptor proteins can be mimicked by chemically sophisticated hosts with well-organised binding sites or, alternatively, by slightly hydrophilic synthetic macromolecules with a chemically simple receptor moiety. The latter approach has been scarcely explored, though it has shown promising results in the selective recognition of anionic species in water solutions (*6*, *8–11*, *13–18*). For example, rectangular strips were prepared with polymethacrylate with a pendant pyrylium substructure, showing excellent colorimetric selectivity towards hydrogen carbonate in water. Remarkably, the colour changes in the presence of the anion were observed only in the slightly water-swelled polymeric matrix, and there was no change upon addition of the anion to an aqueous solution of the pyrylium monomer (*14*, *18*). Polymers with host moieties are not only excellent supports but also allow fine alterations of their hydrophilic/hydrophobic characters, allowing for the tuning of their sensing ability.

Our work focused on the development of polymeric optical transducers for analyses. In previous articles, we reported on the syntheses and characterisations of polymer materials with the following host units: crown ether (*19–21*), urea (*22–25*) or pyrylium (*13*, *18*), along with

*Corresponding author. Email: jmiguel@ubu.es

ISSN 1061-0278 print/ISSN 1029-0478 online

DOI: 10.1080/10610270903531549
http://www.informaworld.com

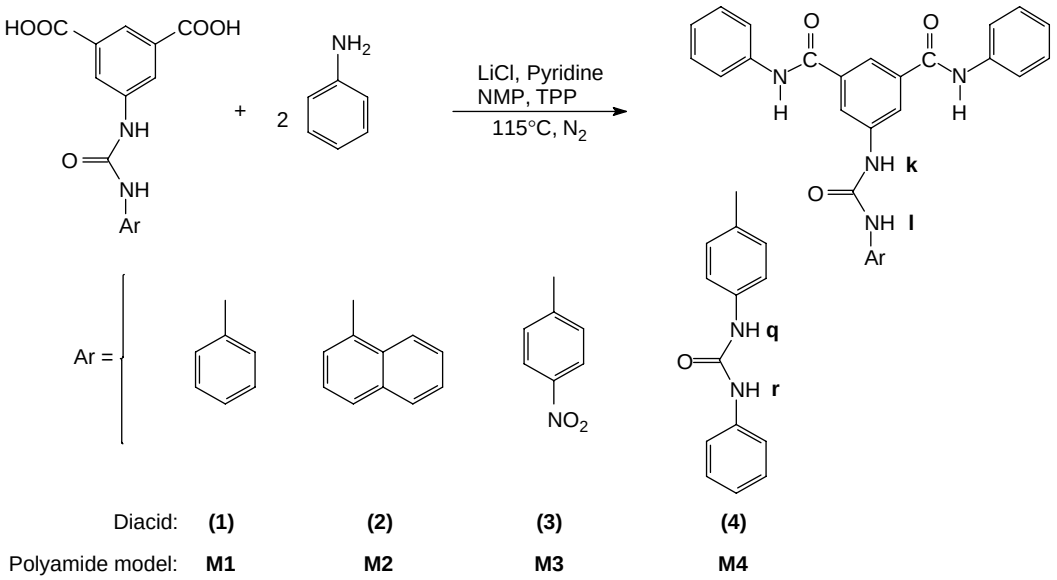

Scheme 1. Synthesis, chemical structure and codes of the polyamide models.

their interaction with cations (*26–31*), anions (*13*, *18*) or gas molecules (*32*). Herein, we report four polyamide model compounds (Scheme 1) that exhibit sensing selectivities towards acetate ions; one of these showed colorimetric sensing capabilities towards acetate anions. The models probably mimic polyamides (Scheme 2, **P1**–**P4**), polymers derived from diacid monomers (**1**–**4**), which are intermediates in the synthesis of the models. The polymeric materials are supposed to retain the ability to interact selectively with these diamines, such that cheap future sensing devices might be user-friendly naked-eye polyamide film sensors or incorporate a polyamide coating at the end of an optic fibre connected to a portable UV–vis diode-array detector. Moreover, the aromatic polyamides are a class of polymers with great technological importance, due mainly to their mechanical and electrical properties and outstanding thermal resistances (*13*, *33*). Thus, sensing devices prepared using these materials could be utilised in a wide range of thermal and mechanical conditions. These properties make them unique

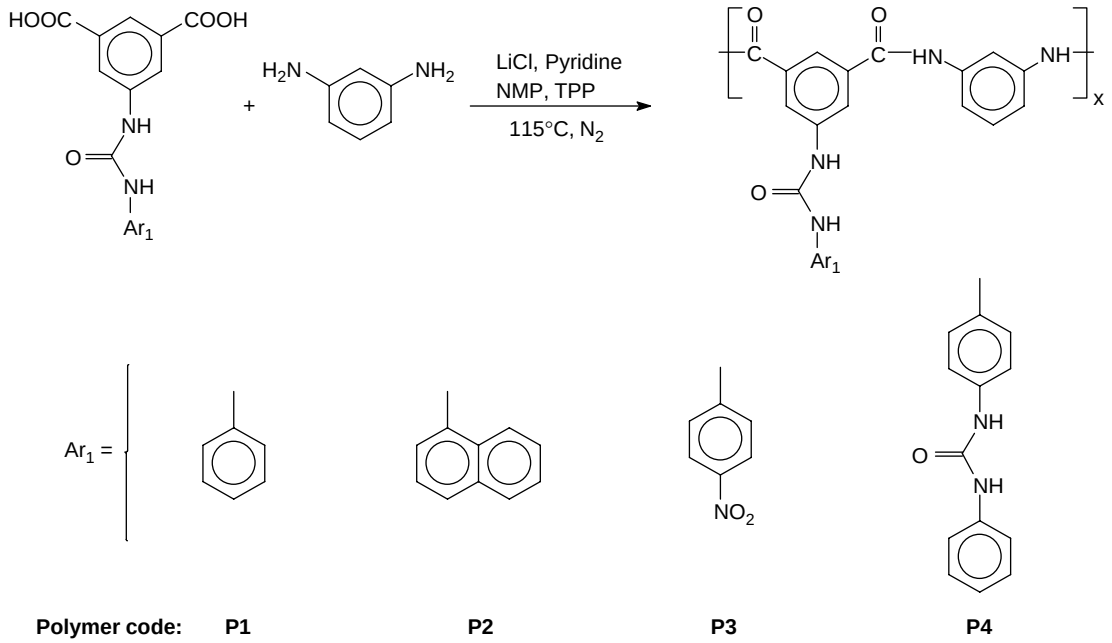

Scheme 2. Synthesis, chemical structure and identification of the polyamides.

components in the control of industrial chemical concentrations, such as in air, gases, reactors or waste products. They also have potential in environmental protection and occupational safety and health, through the determination of chemical concentrations.

2. Experimental

All materials and solvents were commercially available and used as received, unless otherwise indicated. *N*-Methyl-2-pyrrolidone (NMP) was vacuum-distilled twice over phosphorous pentoxide, and then stored in the presence of 4 Å molecular sieves. Lithium chloride was dried at 400°C for 12 h prior to use. Triphenylphosphite (TPP) was vacuum-distilled twice over calcium hydride, and then stored in the presence of 4 Å molecular sieves. Pyridine was dried under reflux over sodium hydroxide for 24 h, and distilled over 4 Å molecular sieves. 5-(3-Phenylureido)isophthalic acid (**1**), 5-(3-naphthylureido)isophthalic acid (**2**), 5-(3-(4-nitrophenyl)-ureido)isophthalic acid (**3**) and 5-(3-(4′-ureidophenyl)-ureidophenyl)isopthalic acid (**4**) were prepared by previously described procedures (*22*).

The following salts were used as received in the complexation studies: sodium hydroxide (98%; Panreac, Barcelona, Spain), tetrabutylammonium fluoride hydrate (98%; Sigma-Aldrich, St Louis, MO, USA), sodium bicarbonate (99.5%; Sigma-Aldrich), lithium phosphate (99%; Sigma-Aldrich), lithium acetate (99.99%; Sigma-Aldrich), lithium benzoate (99%; Sigma-Aldrich), potassium oxalate monohydrate (puriss.; Riedel-de Haën, Seelze, Germany), sodium *p*-toluenesulphonate (95%; Sigma-Aldrich), sodium chloroacetate (98%; Sigma-Aldrich), lithium dihydrogenphosphate (99%; Sigma-Aldrich), lithium trifluoroacetate (95%; Sigma-Aldrich), lithium bromide (puriss.; Riedel-de Haën), sodium methanesulphonate (98%; Sigma-Aldrich), lithium chloride (anhydrous puriss.; Sigma-Aldrich) and tetrabutylammonium iodide (99%; Sigma-Aldrich). Thus, the anion-binding studies were carried out using different counterions (lithium, sodium, potassium and tetrabutylammonium). The solvents used in the complexation studies were dry dimethyl sulphoxide (DMSO, 99%; Merck, Darmstadt, Germany) or dry DMSO-d_6 (deuteration degree min. 99.8%; Merck).

2.1 Polyamide model synthesis

2.1.1 *N,N′-Diphenyl-5-(3-phenyl-ureido)-isophthalamide model (**M1**)*

In a 50 ml three-necked flask fitted with a mechanical stirrer, 20 mmol of aniline, 10 mmol of 5-(3-phenyl-ureido)isophthalic acid and 1.4 g of lithium chloride were dissolved in a mixture of 6 ml of pyridine, 22 mmol of TPP and 20 ml of NMP. The solution was stirred and heated at 110°C under a dry nitrogen blanket for 4 h. Then, the system was cooled at room temperature and the solution was precipitated in 300 ml of methanol. The compound obtained was filtered and washed with distilled water and acetone. Then, it was extracted with acetone for 24 h in a Soxhlet, and dried in a vacuum oven at 80°C overnight (yield, 94%). It was obtained as a semi-crystalline solid (55% crystallinity) that crystallised at 169°C. Mp: 256°C. Tg: 122°C. ^{1}H NMR (400 MHz, DMSO-d_6): δ (ppm), 10.48 (s, 2H); 9.16 (s, 1H); 8.85 (s, 1H); 8.23 (s, 2H); 8.17 (s, 1H); 7.86 (d, $J = 8.3$ Hz, 4H); 7.55 (d, $J = 7.9$ Hz, 2H); 7.42 (m, 4H); 7.35 (m, 2H); 7.17 (t, $J = 7.7$ Hz, 2H); 7.04 (t, $J = 7.3$ Hz, 1H). ^{13}C NMR (100.6 MHz, DMSO-d_6): δ (ppm), 166.21; 153.51; 141.11; 140.39; 140.03; 136.94; 129.79; 129.66; 124.77; 123.11; 121.28; 120.93; 119.40. EI-LR-MS *m/z*: 331 (55), 239 (100), 185 (11), 119 (60), 93 (62), 65 (16). FT-IR [wavenumbers (cm^{-1})]: ν_{N-H}: 3290; $\nu_{C=O}$: 1663, 1651; δ_{N-H}: 1598; $\nu_{ArC=C}$: 1541.

5-(3-Naphthalen-1-yl-ureido)-*N*,*N′*-diphenyl-isophthalamide (**M2**), 5-[3-(4-nitro-phenyl)-ureido]-*N*,*N′*-diphenyl-isophthalamide (**M3**) and *N*,*N′*-diphenyl-5-{3-[4-(3-phenyl-ureido)-phenyl]-ureido}isophthalamide (**M4**) were prepared and purified in a similar manner to that of **M1**.

M2 was obtained as an amorphous solid that crystallised at 204°C. Yield: 92%. Mp: 256°C. Tg: 130°C. ^{1}H NMR (400 MHz, DMSO-d_6): δ (ppm), 10.50 (s, 2H); 9.56 (s, 1H); 8.94 (s, 1H); 8.26 (s, 2H); 8.17 (s, 2H); 8.05 (d, $J = 7.5$ Hz, 1H); 7.99 (d, $J = 8.1$ Hz, 1H); 7.84 (d, $J = 7.8$ Hz, 4H); 7.75–7.50 (m, 4H); 7.42 (m, 4H); 7.17 (t, $J = 7.5$, 2H). ^{13}C NMR (100.6 MHz, DMSO-d_6): δ (ppm), 166.18; 153.94; 141.15; 140.02; 136.99; 134.96; 134.67; 129.63; 129.39; 127.15; 126.91; 126.80; 126.78; 124.74; 124.36; 122.32; 121.27; 121.19; 120.96; 118.92. EI-LR-MS *m/z*: 331 (56), 239 (100), 185 (19), 169 (37), 143 (75), 115 (33), 93 (48), 65 (30). FT-IR [wavenumbers (cm^{-1})]: ν_{N-H}: 3272; $\nu_{C=O}$: 1683, 1649; δ_{N-H}: 1598; $\nu_{ArC=C}$: 1537.

M3 was obtained as a semi-crystalline solid (50% crystallinity) that crystallised at 201°C. Yield: 87%. Mp: 271°C. Tg: 157°C. ^{1}H NMR (400 MHz, DMSO-d_6): δ (ppm), 10.49 (s, 2H); 9.63 (s, 1H); 9.42 (s, 1H); 8.28–8.23 (m, 5H); 7.86–7.78 (m, 6H); 7.42 (m, 4H); 7.17 (t, $J = 7.5$ Hz, 2H). ^{13}C NMR (100.6 MHz, DMSO-d_6): δ (ppm), 166.06; 153.05; 147.10; 142.19; 140.45; 139.99; 136.97; 129.66; 126.12; 124.81; 121.82; 121.58; 121.29; 118.72. EI-LR-MS *m/z*: 331 (37), 239 (61), 185 (11), 164 (35), 138 (85), 119 (57), 108 (51), 91 (56), 78 (42). FT-IR [wavenumbers (cm^{-1})]: ν_{N-H}: 3425; $\nu_{C=O}$: 1721, 1668; δ_{N-H}: 1597; $\nu_{ArC=C}$: 1540; ν_{NO_2}(As,S): 1552, 1329.

M4 was obtained as a crystalline solid. Yield: 91%. Mp: 291°C. Tg: not observed. ^{1}H NMR (400 MHz, DMSO-d_6): δ (ppm), 10.48 (s, 2H); 9.11 (s, 1H); 8.73 (s, 1H); 8.66 (s, 1H); 8.61 (s, 1H); 8.23 (s, 2H); 8.16 (s, 1H); 7.85 (d, $J = 8.0$ Hz, 1H); 7.52–7.39 (m, 10H);

7.32 (m, 2H); 7.17 (t, $J = 7.3$ Hz, 2H); 6.99 (t, $J = 7.2$ Hz, 1H). ^{13}C NMR (100.6 MHz, DMSO-d_6): δ (ppm), 166.23; 153.60; 153.58; 141.26; 140.79; 140.04; 136.93; 135.34; 134.70; 129.73; 129.66; 124.76; 122.63; 121.27; 121.23; 120.79; 120.28; 119.92; 119.06. EI-LR-MS *m/z*: 357 (19), 331 (56), 265 (31), 239 (100), 227 (28), 185 (12), 134 (42), 119 (57), 108 (41), 93 (61). FT-IR [wavenumbers (cm^{-1})]: ν_{N-H}: 3342; $\nu_{C=O}$: 1669, 1648, 1636; δ_{N-H}: 1599; $\nu_{ArC=C}$: 1561.

The polyamide model syntheses and codes are depicted in Scheme 1.

2.2 Polyamide synthesis, characterisation and membrane preparation

The reaction of the diacids (**1**–**3**; Scheme 1) with *m*-phenylenediamine yielded polyamides, as depicted in Scheme 2. The polymerisation and the polymer characterisation were performed following previously described procedures (*22*).

The dense polyamide membranes were prepared by casting an *N*,*N*-dimethylformamide (DMF) solution containing about 8 wt% of the corresponding polymer on glass plates. The membranes were then dried in an oven at 70°C for 4 h. After removing the membranes from the glass plates by distilled water, they were vacuum-dried for 24 h at room temperature and reduced pressure. The resulting yellowish transparent dense membranes had a thickness of 20–50 μm.

The skinned asymmetric membranes were prepared by the phase inversion precipitation method. The polymeric solutions consisted of 15–20 wt% of cellulose acetate (39.8 wt% acetyl content, average Mn ~30,000; Aldrich, St Louis, MO, USA), 10 wt% of the corresponding polyamide and 70–75 wt% of DMF as the solvent. The polymer solutions were cast onto glass plates and subsequently immersed in a 25 ± 1°C water/DMF coagulation bath (up to 30% v/v of DMF). The membrane was peeled off from the glass plate, washed for 12 h with water to remove all solvents, dried at room temperature for 24 h and dried further at reduced pressure for 48 h.

2.3 Measurements and instrumentation

The ^{1}H and ^{13}C NMR spectra were recorded using a Varian Inova 400 spectrometer operating at 399.92 and 100.57 MHz, respectively, with DMSO-d_6 as the solvent.

Fast atom bombardment and low-resolution electron impact mass spectra (EI-LR-MS, 70 eV) were measured on a Micromass AutoSpec Waters mass spectrometer.

Infrared spectra (FT-IR) were recorded using a Nicolet Impact spectrometer.

The UV–vis spectra were recorded using a Varian Cary3-Bio UV–vis spectrophotometer.

Differential scanning calorimetry data were recorded on a Perkin-Elmer Pyris I analyser from 10 mg of sample under a nitrogen atmosphere at a scan rate of 20°C/min.

The membrane cross-section was observed by means of scanning electron microscopy (SEM). The SEM images were obtained with a JEOL JSM-6460LV, using an accelerating voltage of 20 kV. The polymer samples were cryofractured from film membranes and coated with gold.

Stock solutions of polyamide model compounds and of concentrated solutions of the salts were prepared in DMSO or DMSO-d_6 for the UV–vis and ^{1}H NMR experiments, respectively. Samples were prepared directly in UV–vis cuvettes or in NMR tubes by adding the proper polyamide model compound in the DMSO solution and mixing with small variable volumes of the concentrated salt solutions. Although the total volume variation was negligible, it was considered in the analysis of the UV–vis spectra. Potassium oxalate and lithium trifluoroacetate were not soluble in DMSO, so water solutions were used instead of DMSO solutions. This situation is troublesome because water competes effectively with the urea groups, giving rise to solvated anions, which are unfavourable for creating host:guest complexes. Therefore, the results with these anions may be questionable.

3. Results and discussion

Four polyamide model compounds were prepared following simple and common synthetic procedures (Scheme 1). The new polyamide model compounds contain one or two urea groups and two aromatic amide linkages, in which the carbonyl groups of the amides act as slightly electron-withdrawing groups and the urea moieties act as feeble electron-donating subunits. The urea group is electron-donating because of its resonance effect and is conversely electron-withdrawing due to its field effect. The resonance effect is predominantly observed in the nitration of *N*,*N*′-diphenylurea, during which the urea group directs the nitration mainly to the *para*-positions and slightly to the *ortho*-positions but not to the *meta*-positions (*34*). As an illustrative example, Figure 1 shows the characterisation of **M3**.

Due to their strong hydrogen-bonding ability (*35*–*54*), urea groups have been widely exploited in compounds that exhibit sensing behaviour towards anions, both in solution and the solid state. However, their possibilities in anion-sensing applications have not been completely analysed, partly because of the complex nature of the intermolecular interactions of the urea-containing organic molecules. Aromatic urea derivatives have shown the ability to form oligomeric assemblies, or capsules, in which guests can be encapsulated in solution. These complex capsules persist even in the solid state, as demonstrated by the X-ray analysis by Alajarín et al. (*55*–*57*).

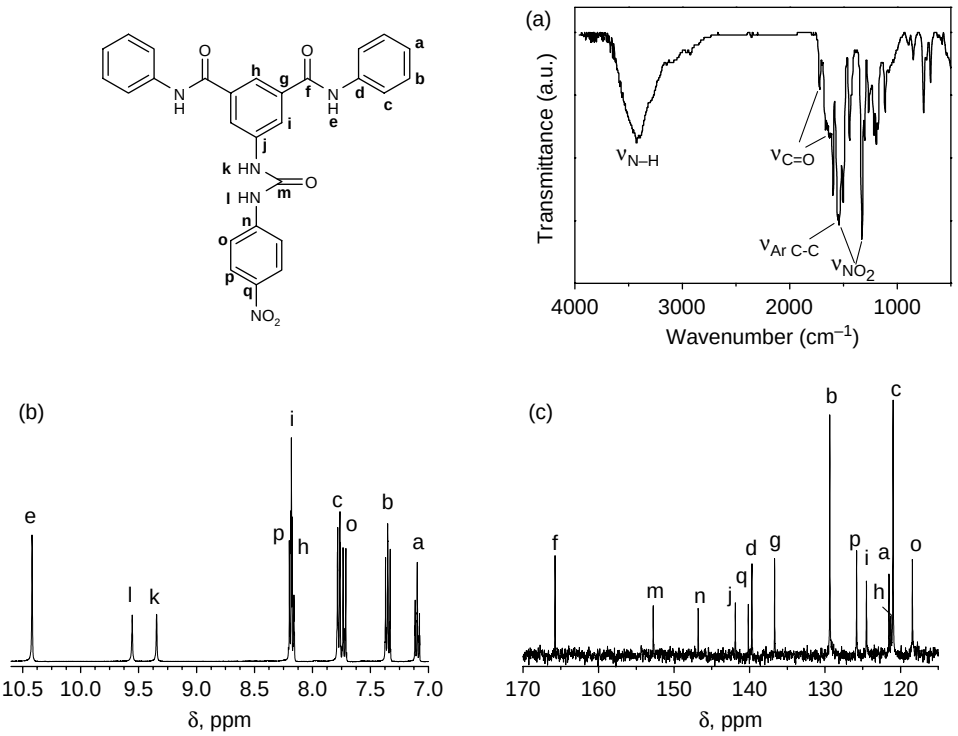

Figure 1. Characterisation of the polyamide **M3** model by (a) FT-IR, (b) ^{1}H NMR and (c) ^{13}C NMR.

The interactions of the model compounds with different anions (OH^-, F^-, HCO_3^-, PO_4^{3-}, AcO^-, benzoate, oxalate, *p*-toluenesulphonate, $CH_2ClCO_2^-$, $H_2PO_4^-$, $CF_3CO_2^-$, Br^-, methanesulphonate, Cl^- and I^-) in solution were evaluated using NMR and UV–vis techniques.

Figure 2 shows the effect of the addition of anions to a solution of **M3** in DMSO, as seen by the naked eye. Colour changes are observed upon addition of (a) AcO^-, benzoate, oxalate and *p*-toluenesulphonate (yellow) and (b) OH^-, F^-, HCO_3^- and PO_4^{3-} (red–orange).

The reddish colour developed upon addition of OH^-, F^-, HCO_3^- and PO_4^{3-} is not due to a host–guest interaction, but to an acid–base reaction. The unsolvated anions behave as strong bases in organic conditions, causing the deprotonation of the urea group and giving rise to a charge transfer complex responsible for the UV–vis absorption band centred at 478 nm. This is a well-known behaviour described by Esteban-Gomez et al. (*58*). As an example, the UV–vis spectrum of the **M3**:F^- system in DMSO is shown in Figure 3. The addition of water causes the disappearance of the charge transfer absorption band ($\lambda_{max} = 490$ nm) and the development of a new absorption band at $\lambda_{max} = 478$ nm, characteristic of the host–guest interactions between the anion (F^-) and the model. The breakage of the strong charge transfer complex, giving rise to the host–guest complex upon water addition, can be monitored by the appearance of an isosbestic point

Figure 2. Photograph of **M3** solutions in DMSO ([**M3**] = 2×10^{-3} M). (a) Upon addition of complexing anions, from left to right: control blank, acetate, benzoate, oxalate, *p*-toluenesulphonate, chloroacetate, dihydrogen phosphate, trifluoroacetate, bromide, methanesulphonate, chloride and iodide. (b) Upon addition of basic anions producing deprotonation of the urea group, from left to right: control blank, OH^-, F^-, HCO_3^- and PO_4^{3-}.

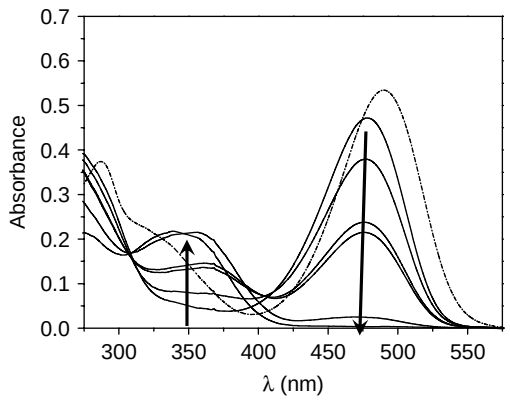

Figure 3. UV–vis spectra of **M3** in DMSO ($[\mathbf{M3}] = 3 \times 10^{-5}$ M) with 10 equivalents of F^- without water (dashed line) and with different water contents (solid lines). The arrows show the trend of the absorption bands with increasing quantities of water.

(Figure 3; 305 nm), corresponding to the different concentration of the **M3**:F^- complex. The disappearance of the urea proton signal in the ^{1}H NMR spectra of **M3** in DMSO-d_6 solution upon addition of F^- is in agreement with the deprotonation of urea and the formation of the strong charge transfer push–pull complex. Figure 4 shows the UV–vis spectra of **M3** solutions with acetate, benzoate, oxalate and fluoride anions.

The other model compounds, **M1**, **M2** and **M4**, do not show a colorimetric response towards anions, although they exhibit complexing abilities towards anions, as detected by UV–vis and ^{1}H NMR spectra. The differences between these models and **M3** arise from the strong electron-withdrawing nitro group in the 4-nitrophenyl-ureido moiety in the latter.

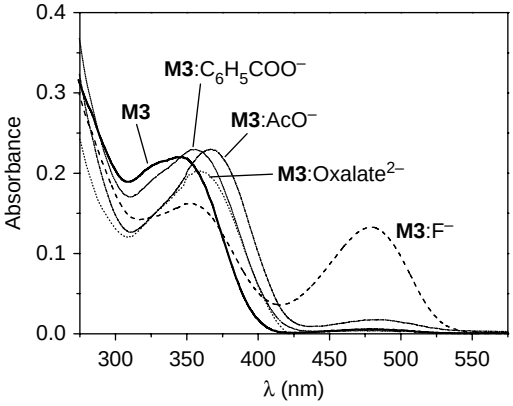

Figure 4. UV–vis spectra of **M3** solutions in DMSO ($[\mathbf{M3}] = 2 \times 10^{-5}$ M) with 10 equivalents of fluoride, acetate, benzoate and oxalate. The spectra of the **M3** solutions with 10 equivalents of *p*-toluenesulphonate, methanesulphonate, trifluoroacetate and chloroacetate are indistinguishable from the initial solution. The solid line represents the spectrum of **M3** in DMSO without salts.

3.1 Titration of the acetate ion in an M3 solution in DMSO

The UV–vis spectrum of **M3** in a DMSO solution shows an absorption maximum around 346 nm, giving rise to a light beige solution. Upon addition of lithium acetate, the solution turns golden yellow due to the displacement of the λ_{max} to higher wavelengths (Figure 5). The magnitude of the displacement can be correlated with the molar ratio of **M3** to acetate ions, allowing for a titration of acetate ions with a detection limit of approximately 100 ppb. A more correct titration curve can be obtained by monitoring the absorbance at 367 nm and plotting these values as a function of the acetate concentration in a DMSO solution of **M3** (5×10^{-5} M) (Figure 5). From the curve-fitting equations, values of the acetate concentration can be obtained as a function of the λ_{max} or the absorbance at 367 nm. Acetate concentrations between 65 and 610 ppb could be estimated by both calculations with mean errors of 8 and 11%, respectively, and with a mean error of 6% when combining both calculations.

3.2 Titration of the acetate ion by the displacement of fluoride from its binding complex with M3 in DMSO

Efficient displacement of fluoride in the host:guest **M3**:F^- complexes was observed by titration with acetate. The red solution of **M3**:F^- in DMSO turns yellow upon addition of increasing quantities of acetate (Figure 6), indicating the displacement of the fluoride anion.

Figure 6 shows the UV–vis spectra of a DMSO solution of **M3**:F^- (1:1) with increasing concentrations of acetate. Fitting the curve of the acetate:**M3** ratio, which is equal to the acetate:F^- ratio vs. the absorbance at 364 and 479 nm (Figure 7) allows for the calculation of the acetate concentration once the absorbance is known. The calculated acetate concentrations in the range of 0.6–2.6 ppm had a mean error of 3%, whereas the mean error for calculated anion concentrations between 5 ppb and 3 ppm was 7%. The latter range of acetate concentrations corresponds to a ratio of **M3**:F^-:AcO^- of 1:1:1.

The driving force of the process is largely dependent on the strong acetate:urea interaction (Table 1). The proton mobility associated with the acid–base reaction of the urea group and the naked fluorine anion is restricted by the double hydrogen bond of the acetate ion/urea (see the chemical structure in Figure 9, inset). The acetate counterion (Li^+) could also play a role in the stabilisation of the fluoride anion, giving rise to ion pairs.

3.3 Analysing the host:guest interactions by stability constants

The strength of the interaction of the anions (acetate, benzoate, oxalate, *p*-toluenesulphonate, trifluoroacetate

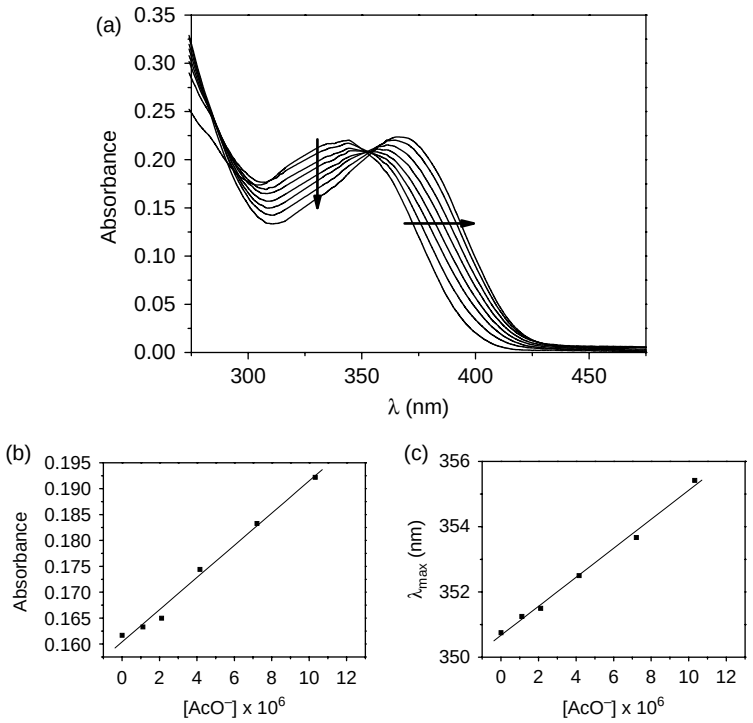

Figure 5. (a) UV–vis spectra of solutions of **M3**:acetate ([**M3**] = 2×10^{-5} M). The arrows indicate the spectra obtained upon increasing the acetate concentration from a **M3**:acetate ratio of 1:0 to 1:10. (b) Titration curves of acetate at 367 nm vs. acetate concentration. (c) λ_{max} vs. acetate concentration.

and chloroacetate) with the polyamide models in DMSO solution was analysed in terms of their stability constants by ^{1}H NMR (*59–63*).

To get insight into the interactions between anions and models in solution, ^{1}H NMR spectra of the models in DMSO-d_6 (0.05 M) were measured at 20°C with the addition of increasing quantities of the anions. Upon addition of the anions, chemical shifts of the protons of the urea groups to lower magnetic fields were observed (see Figures 8 and 9 for the **M3**:acetate system). The graphical representation of the displacements of the chemical shifts of the **M3** model upon addition of different quantities of acetate ions (Figure 9) clearly points to the formation of a 1:1 complex (model:anion). The same behaviour was observed for models **M1** and

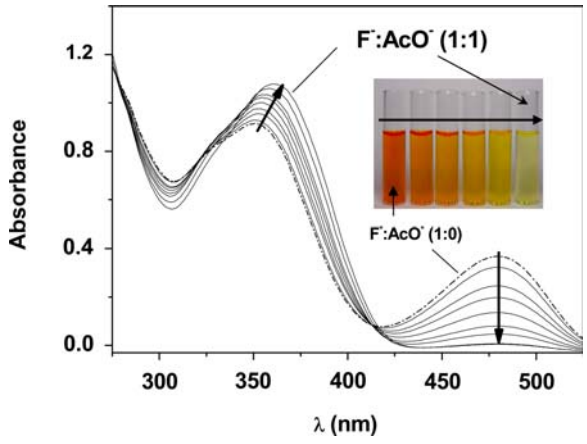

Figure 6. UV–vis spectra of **M3**:F^- (1:1) solutions in DMSO upon adding increasing quantities of acetate ions to reach a ratio of **M3**:F^-:AcO^- of 1:1:4. Inset: photograph depicting titration. The figure depicts the ratio of fluoride to acetate, with the arrows indicating increasing concentrations of acetate. The dashed line corresponds to the initial spectrum of **M3**:F^- (1:1) without acetate. The concentrations of **M3** and fluoride were 5×10^{-5} M.

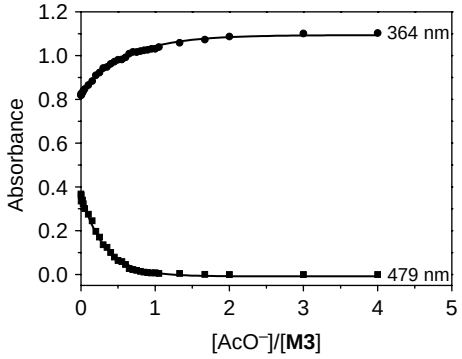

Figure 7. Absorbance of DMSO solutions of **M3**:F^- (1:1) at a given wavelength upon addition of increasing quantities of acetate ions, reaching a ratio of **M3**:F^-:AcO^- of 1:1:4. The concentration of **M3** was 5×10^{-5} M.

Table 1. Stability constants (K_1) corresponding to the interaction of models **M1**–**M3** with selected anions obtained upon application of Equation (9) (for proton assignment see Scheme 1).

Anion	Urea proton *k*		Urea proton *l*	
	K_1	$\Delta\delta_{AM}$	K_1	$\Delta\delta_{AM}$
	M1 model[a]			
Benzoate	358±115	3.19±0.08	344±114	3.09±0.08
Acetate	6641±4378	3.18±0.03	6553±4800	3.11±0.03
Trifluoroacetate	218±96	0.47±0.02	198±80	0.51±0.02
Oxalate	16±2	1.25±0.04	16±2	1.29±0.04
	M2 model[a]			
Benzoate	127±14	2.84±0.04	113±11	2.46±0.03
Acetate	385±192	2.71±0.09	340±154	2.45±0.08
Trifluoroacetate	16±3	0.71±0.04	15±3	0.64±0.04
Oxalate	–[b]	0.09[b]	–[b]	0.06[b]
	M3 model[a]			
Benzoate	647±245	3.63±0.03	691±232	3.56±0.05
Acetate	28889±8317	3.68±0.01	21516±8120	3.59±0.08
p-Toluenesulphonate	11.8±0.8	0.54±0.01	13±1	0.51±0.02
Oxalate	–[b]	0.48[b]	–[b]	0.45[b]
Chloroacetate	33±3	1.71±0.04	28±3	1.45±0.03

[a] The trifluoroacetate and oxalate anions did not fit well to the mathematical model, because of the small water content of the measurement solutions. The salts were insoluble in DMSO, therefore requiring them to be added as concentrated water solutions.
[b] The stability constants are too low to be accurately measured ($\Delta\delta_{AM}$ values are experimental values).

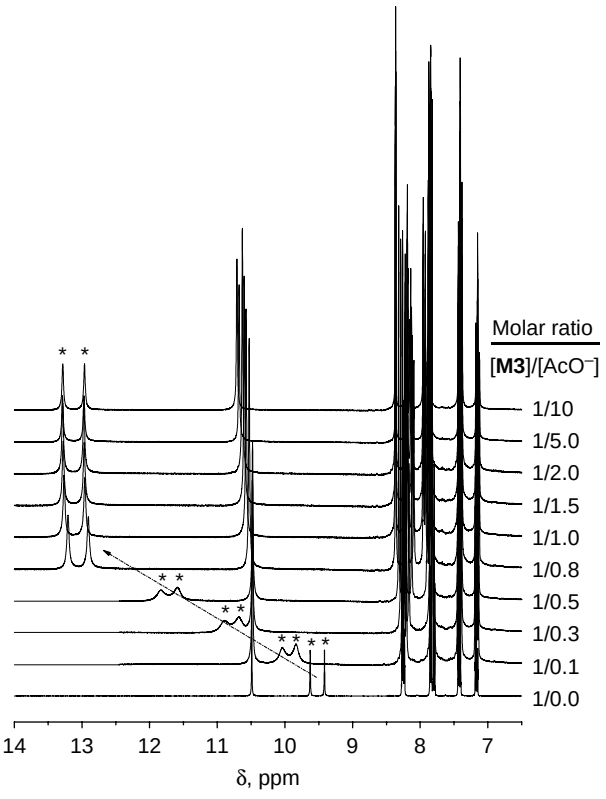

Figure 8. ^{1}H NMR spectra of the **M3**:lithium acetate system at different molar ratios of **M3** to acetate ion (solvent, DMSO-d_6; [**M3**] = 5×10^{-2} M; *, urea proton signals).

M2 with all the studied anions. However, the presence of two urea moieties in the **M4** model gave rise to 1:2 complexes.

The urea protons of the **M3** model in DMSO-d_6 showed sharp ^{1}H NMR signals. Upon addition of acetate, the signal broadened, indicating a fast exchange of the acetate between different urea groups when the **M3**:acetate ratio is low (lower than 1:0.8). Upon increasing the acetate concentration to a ratio of 1:1, the signals became sharp again, indicating a low mobility of the ion and a strong stability constant, with a negligible free acetate concentration in solution.

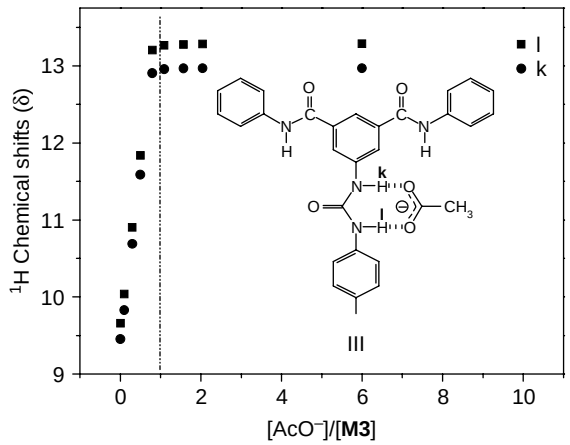

Figure 9. Chemical shifts of the urea protons vs. acetate to **M3** molar ratio ([**M3**] = 5×10^{-2} M).

The stoichiometry of the anion:metal complexes have been mathematically determined by studying the chemical shift displacements of the urea protons (as determined from ^{1}H NMR experiments) vs. the anion concentration and their corresponding Job's plots for the following anions: acetate, benzoate, trifluoroacetate, chloroacetate, *p*-toluenesulphonate and oxalate. Job's plots of **M1**–**M3** have a maxima appearing at $X_H = 0.5$, clearly indicating the formation of complexes with a 1:1 stoichiometry with the different anions, even with the divalent oxalate. Conversely, the maxima of **M4** were found at 0.33, pointing to complexes with 1:2 stoichiometry (model to anions). As an illustrative example, Figure 10 depicts the chemical shift displacements and Job's plots corresponding to the interaction of the benzoate anion with the models.

With the stoichiometry of the complexes known, the dimensionless stability constants of the formation of an *n*:*m* complex (M_mA_n) between the anion (A) and the model (M) can be determined by

$$mM + nL \leftrightharpoons M_mA_n, \quad K_{nm} = \frac{[M_mA_n]}{[M]^m[L]^n}. \tag{1}$$

We studied the interaction of the models with benzoate, acetate, trifluoroacetate, chlorobenzoate, *p*-toluenesulphonate and oxalate. As previously outlined, the **M1**–**M3** models have a 1:1 stoichiometry, whereas **M4** is characterised by a 1:2 (**M4**:anion) stoichiometry.

The study of the complex formation between each model:anion pair was performed following the chemical shift variations of the proton signals *k*, *l*, *q* and *r* (Scheme 1) of the models in DMSO-d_6 at 20°C with increasing anion concentrations.

The 1:1 complex formation between the host (model) and the guest (anion) is represented by Equation (2), where M represents the model, A represents the anion and MA represents the complex with a 1:1 stoichiometry.

$$M + A \leftrightharpoons MA. \tag{2}$$

Thus, the stability constant is given by Equation (3):

$$K_1 = \frac{[MA]}{[M][A]}. \tag{3}$$

Under fast-exchange conditions (*59*), the observed chemical shift for a model can be expressed by Equation (4):

$$\Delta\delta_{obs} = \chi_M\delta_M + \chi_{MA}\delta_{MA}, \tag{4}$$

where δ_M and δ_{MA} represent the chemical shift of the free and complexed models, respectively, and χ_M and χ_{MA} are their molar fractions. From the mass balance, the observed chemical shifts can be expressed as $\Delta\delta_{obs} = \delta_{obs} - \delta_M$ and $\Delta\delta_{MA} = \delta_{MA} - \delta_M$. Equation (5) is deduced from Equation (4):

$$\Delta\delta_{obs} = \frac{\Delta\delta_{MA}}{[M]_0}[MA], \tag{5}$$

where $[M]_0$ is the initial concentration of model M. The mass balances of M and A are given by

$$[M]_0 = [M] + [MA] \tag{6}$$

and

$$[A]_0 = [A] + [MA]. \tag{7}$$

Considering Equation (3) and the mass balances of M and A (Equations (6) and (7)), the complex concentration can be solved as a function of K_1 and the initial concentrations of M and A:

$$[MA]^2 - \left([A]_0 + [M]_0 + \frac{1}{K_1}\right)[MA] + [A]_0[M]_0 = 0. \tag{8}$$

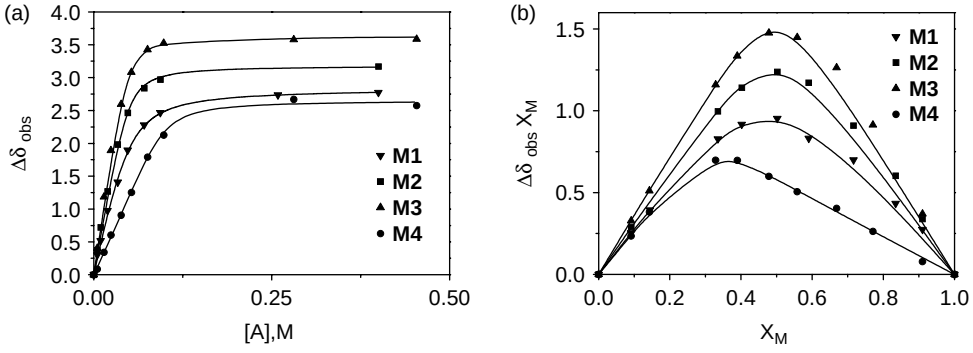

Figure 10. (a) Plot of the observed chemical shift displacements, $\Delta\delta$, of the urea protons vs. benzoate concentration. (b) The corresponding Job's plot. Solid lines are the results of fitting and applying the corresponding equations.

From Equations (3) and (8), Equation (9) is deduced as

$$\Delta\delta_{obs} = \frac{\Delta\delta_{MA}}{[M]_0}\left\{\left([A]_0 + [M]_0 + \frac{1}{K_1}\right) - \sqrt{\left([A]_0 + [M]_0 + \frac{1}{K_1}\right)^2 - 4[A]_0[M]_0}\right\}, \quad (9)$$

which relates the experimental $\Delta\delta_{obs}$ with the $[A]_0$. Thus, the experimental data can be fitted using a nonlinear least-squared algorithm (*64*) to obtain the parameters K_1 and $\Delta\delta_{MA}$.

The stability constants of the 1:1 complexes were calculated for **M1**–**M3** with Equation (9) separately using the chemical shifts of the two urea protons (*k* and *l*; Scheme 1). The results (Table 1) show that the stability constants calculated using both proton signals are equivalent, as expected, confirming the validity of the calculation model.

The host–guest analyses performed by the 'naked-eye' and the UV–vis technique confirmed that the addition of acetate ions to a solution of **M3** in DMSO gave rise to the stronger colour changes. The stability constants for each model obtained by the ^{1}H NMR analyses revealed that the acetate anion has the strongest interaction for all of the models in DMSO. The strength of the different complexes is related to the electron density surrounding the urea group. Thus, the high electron-withdrawing capability of the nitro group through inductive and mesomeric effects withdraws electron density from the urea group, giving rise to the higher stability constants of the **M3**:anion complexes. Furthermore, the strength of the interaction of the carboxylate anions with a specific model depends inversely on the pK_a of their conjugated bases in DMSO (*65*), thus the association depends inversely on the localisation of the negative charge over the carboxylic group because of the mesomeric effect and the electron density due to inductive effects.

The order of stability constants of the model:acetate complexes (**M3**:acetate > **M1**:acetate > **M2**:acetate) is in agreement with theoretical calculations (*ab initio*). Therefore, gas-phase density functional theory calculations at the B3LYP/6-31G* level of theory were performed following a previously described procedure (*31*, *66*). The interaction energies of the acetate ion with simplified models of **M1**–**M3** (i.e. diphenylurea, 1-(naphthalen-2-yl)-3-phenylurea and 1-(4-nitrophenyl)-3-phenylurea) were −224, −219 and −266 kJ/mol, respectively.

If we consider a 1:2 complex formation between the host (**M4** model) and the guest (anion), the complex formation can be represented by Equations (10) and (11):

$$M + A \leftrightharpoons MA, \quad K_1 = \frac{[MA]}{[M][A]} \quad (10)$$

and

$$MA + A \leftrightharpoons MA_2, \quad K_2 = \frac{[MA_2]}{[MA][A]}, \quad (11)$$

where K_1 and K_2 are stability constants of the complexes. The mass balances are expressed as

$$[M]_0 = [M] + [MA] + [MA_2] \quad (12)$$

and

$$[A]_0 = [A] + [MA] + 2[MA_2]. \quad (13)$$

Considering the stability constant, Equations (10) and (11) and the mass balances of M and A (Equations (12) and (13)), Equation (14) can be deduced as

$$K_1K_2[A]^3 + (K_1K_2(2[M]_0 - [A]_0) + K_1)[A]^2 + (K_1([M]_0 - [A]_0) + 1)[A] + [A]_0 = 0. \quad (14)$$

Given the concentration of [A], the equilibrium concentrations of M, MA and MA_2 can be calculated

Table 2. Stability constants (K_1 and K_2) corresponding to the interaction of **M4** with selected anions (for proton assignment see Scheme 1).

Anions	K_1	K_2	$\Delta\delta_{AM}$	$\Delta\delta_{MA_2}$	K_1	K_2	$\Delta\delta_{AM}$	$\Delta\delta_{MA_2}$
	Urea proton *k*				Urea proton *l*			
Benzoate	379	85	2.3	2.99	436	80	2.15	2.83
Acetate	778	1.1	2.77	3.05	774	0.4	2.65	3.13
p-Toluenesulphonate	14	2.9	0.23	0.44	23	2.2	0.21	0.56
	Urea proton *q*				Urea proton *r*			
Benzoate	424	121	1.19	2.66	424	121	1.17	2.63
Acetate	0.005	101	1.71	2.41	0.005	97	1.67	2.35
p-Toluenesulphonate	27	1.2	0.18	0.72	27	1.1	0.18	0.71

Note: The stability constants corresponding to the **M4**:oxalate complex are too low to be accurately measured and are not depicted in the table.

Table 3. Stability constants (K_1 and K_2) corresponding to the interaction of **M4** with acetate calculated from the 1:1 interaction model for each urea group using Equation (9) (for proton assignment see Scheme 1).

	Urea proton *k*	Urea proton *l*	Urea proton *q*	Urea proton *r*
K_1	528±93 (778)	557±119 (774)	97±25 (101)	98±24 (97)

Note: For comparison, we included the values obtained by the 2:1 model (Equation (19)) in parentheses.

as described by Al-Soufi et al. (*60*):

$$[M] = \frac{[M]_0}{1 + K_1[A] + K_1K_2[A]^2}, \quad (15)$$

$$[MA] = K_1[A][M] \quad (16)$$

and

$$[MA_2] = K_2[MA][A]. \quad (17)$$

The observed chemical shift of a proton, δ_{obs}, is given by the following equation:

$$\Delta\delta_{obs} = \chi_M\delta_M + \chi_{MA}\delta_{MA} + \chi_{MA_2}\delta_{MA_2}, \quad (18)$$

where δ_M, δ_{MA} and δ_{MA_2} represent the chemical shifts of the free and complexed forms of the model, and χ_M, χ_{MA} and χ_{MA_2} are their molar fractions, respectively. From Equations (12) and (18), the following expression can be deduced:

$$\Delta\delta_{obs} = \frac{\Delta\delta_{MA}}{[M]_0}[MA] + \frac{\Delta\delta_{MA_2}}{[M]_0}[MA_2]. \quad (19)$$

As has been previously outlined for a 1:1 stoichiometry, Equation (19) can be fitted to experimental data considering Equations (14)–(17) and using a nonlinear least-squared algorithm (*67*) to obtain the parameters K_1, K_2, $\Delta\delta_{MA}$ and $\Delta\delta_{MA_2}$. The results of the stability constants are depicted in Table 2. Upon fitting the data of each urea proton, the two stability constants are sometimes obtained, indicating that the interaction of a single model guest molecule with one of the urea groups can affect the other. This is true for benzoate and *p*-toluenesulphonate, but not for acetate. The distinct behaviour for acetate is reflected in the results obtained using Equation (19) and is shown in Table 2. When we tried to obtain the stability constants with the chemical shifts of one of the urea groups, we obtained a correct value for the constant of the interaction with this group but a value near zero for the other urea group. We believe that this fact is due to the restricted mobility of the acetate anions because of the stronger host:acetate interaction compared to those with other anions. Nevertheless, each constant of **M4**:acetate can be estimated by applying the 1:1 model to each urea group by Equation (9) (Table 3), and the results are similar to those obtained with the 2:1 model.

4. Outlooks

The amide linkages are the key motif of the polyamide backbones, and are naturally present in the polyamide models. Nevertheless, the amide groups do not play an important role in the complexation. The small downfield displacement of the amide protons upon interaction with acetate ions, as observed by ^{1}H NMR (Figure 8), arises from modification of the overall electron density of the molecule due to the interaction of the urea motif with the anions, as can be observed in the chemical shift displacements of the amidic protons vs. acetate to **M3** molar ratio (Figure 11), where it is observed a change in the slope of the curve corresponding to a **M3**:acetate molar ratio of 1:1.

Solutions in DMSO of the polymers prepared upon polymerisation of the diacids **1**–**4** with *m*-phenylenediamine (Scheme 2) retain the ability to interact selectively with anions, as determined by qualitative ^{1}H NMR and 'naked-eye' analyses. However, the addition of water to the solution gives rise to the solvation of the anions with the concomitant loss of the host–guest interactions.

Nevertheless, and in agreement with previous results (*13*, *18*), a membrane with an adequate hydrophilic/hydrophobic balance can partially inhibit the efficient water–anion interaction, giving rise to the recognition event inside the membrane in a solid–liquid interaction, where the solid is a partially water-swelled matter. The water-swelled organic membrane must have enough water content to allow the water-solvated anions to enter the membrane by diffusion. At the same time, this water content should be lower enough to let lipophilic domains inside the

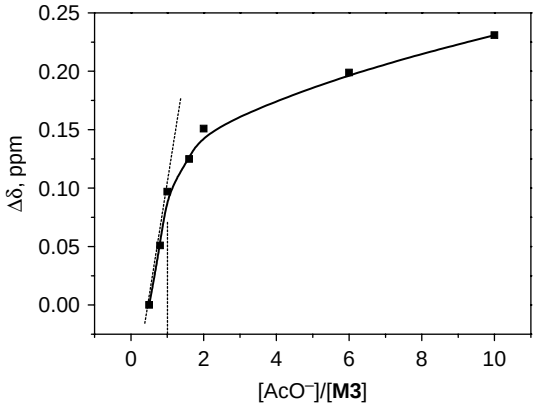

Figure 11. Chemical shifts of the amidic protons vs. acetate to **M3** molar ratio ([**M3**] = 5×10^{-2} M).

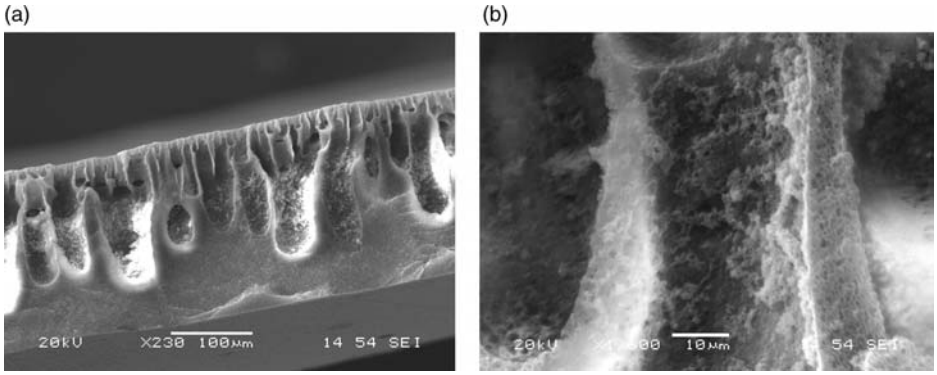

Figure 12. (a) SEM cross-section image of a cellulose acetate/**P3** asymmetric membrane obtained by casting a solution of cellulose acetate/**P3**/DMF (15:10:75, w/w/v) in a water/DMF (70:30, v/v) coagulation bath. (b) Enlargement of a pore.

membrane where the recognition process takes place. In polyacrylate and polymethacrylate networks, membranes with a water uptake of 50% w/w have an optimum balance for anion recognition in pure water.

Dense membranes, or film strips, prepared with polyamides **P1**–**P4** (Scheme 2) were hydrophobic [films prepared with **P3** showed a water uptake of 3.6% at 65% relative humidity (rh)] and remained silent in water media with increasing quantities of anions. In order to increase the hydrophilicity, the films were prepared with a blend of cellulose acetate and **P3** (10% of the latter), achieving a water uptake of 14.5% (at 65% rh).

The blend of the polyamides with cellulose acetate has also been used to obtain asymmetric membranes. The objective was to increase the surface of the materials to test the influence on the recognition processes in water media. The pore control was achieved by means of varying the DMF content of the water/DMF coagulation bath. Figure 12 depicts an SEM photograph of an asymmetric membrane showing large transversal pores and their porous structures.

Both membranes, dense and asymmetric, based on **P3** and cellulose acetate, show a weak 'naked-eye' colorimetric response towards fluoride in water. Thus, white strips obtained with the membranes turned to pale red when immersed in water containing the fluoride ion. Nevertheless, a high concentration of fluoride was needed to observe the phenomenon. Accordingly, further work is needed to obtain positive results with much lower guest concentrations in water environments. One way to achieve this is to increase the hydrophilicity of the system by increasing the water affinity of the polymer to be blended with the polyamides.

5. Conclusions

We have developed new polyamide model compounds that are structurally simple sensors containing the urea receptor group as the selective binding site for anions. One of the models behave as an effective colorimetric probe for carboxylic acid salts, specifically for acetate. The light beige solutions of **M3** in DMSO develop a reddish colour upon addition of basic anions, such as OH^- and F^-, and a yellowish colour upon adding acetate salts. The titration of acetate can be performed by adding the anion to (a) a model solution in DMSO, giving rise to the development of a yellow colour, or (b) a red solution of a mixture of model/fluoride (1:1), turning the reddish solution to yellow due to the displacement of fluoride by the acetate. The host:guest stoichiometry (polyamide model compound:anion complexes) and the stability constants of complexes were determined by ^{1}H NMR. The models mimic polyamides, the polymers derived from the diacid monomers (**1**–**4**), which are intermediates in the synthesis of the models. The polymers retain the ability to interact selectively with anions in organic media, and cheap future sensing devices might take the form of user-friendly naked-eye polyamide film sensors or might incorporate a polyamide coating at the end of an optic fibre connected to a portable UV–vis diode-array detector. Further work is needed to achieve a colorimetric response of the polymer materials in water environments.

Acknowledgements

The financial support provided by the Spanish MICINN (Ministerio de Investigación e Innovación) – FEDER (MAT2008-00946/MAT) and the Caja de Burgos is gratefully acknowledged.

References

(1) Trinchi, A.; Muster, T.H. *Supramol. Chem.* **2007**, *19*, 431–445.
(2) Kim, S.K.; Kim, H.N.; Xiaoru, Z.; Lee, H.N.; Soh, J.H.; Swamy, K.M.K.; Yoon, J. *Supramol. Chem.* **2007**, *19*, 221–227.
(3) Martínez-Máñez, R.; Sancenón, F. *Chem. Rev.* **2003**, *103*, 4419–4476.
(4) Martínez-Máñez, R.; Sancenón, F. *J. Fluoresc.* **2005**, *15*, 267–285.

(5) Sessler, J.L.; Gale, P.A.; Cho, W.S. *Anion Receptor Chemistry*; RSC Publishing: Cambridge, 2006.
(6) Anzenbacher, P.; Jursíková, K.; Aldakov, D.; Marquez, M.; Pohl, R. *Tetrahedron* **2004**, *60*, 11163–11168.
(7) Bosch, P.; Catalina, F.; Corrales, T.; Peinado, C. *Chem. Eur. J.* **2005**, *11*, 4314–4325.
(8) Yoshimura, I.; Miyahara, Y.; Kasagi, N.; Yamane, H.; Ojida, A.; Hamachi, I. *J. Am. Chem. Soc.* **2004**, *126*, 12204–12205.
(9) Mohan, S.R.K.; Hamachi, I. *Curr. Org. Chem.* **2005**, *9*, 491–502.
(10) Kiyonaka, S.; Sada, K.; Yoshimura, I.; Shinkai, S.; Kato, N.; Hamachi, I. *Nat. Mater.* **2003**, *3*, 58–64.
(11) Yamaguchi, S.; Yoshimura, I.; Kohira, T.; Tamaru, S.; Hamachi, I. *J. Am. Chem. Soc.* **2005**, *127*, 11835–11841.
(12) Ojida, A.; Inoue, M.; Mito-oka, Y.; Hamachi, I. *J. Am. Chem. Soc.* **2003**, *125*, 10184–10185.
(13) García, J.M.; García, F.C.; Serna, F.; de la Peña, J.L. *Prog. Polym. Sci.* **2009**, doi:10.1016/j.progpolymsci.2009.09.002.
(14) García-Acosta, B.; García, F.; García, J.M.; Martínez-Máñez, R.; Sancenón, F.; San-José, N.; Soto, J. *Org. Lett.* **2007**, *9*, 2429–2432.
(15) Zyryanov, G.V.; Kinstle, T.H.; Anzenbacher, P. *Synlett* **2008**, 1171–1174.
(16) Aldakov, D.; Anzenbacher, P. *J. Am. Chem. Soc.* **2004**, *126*, 4752–4753.
(17) Kiyonaka, S.; Sugiyasu, K.; Shinkai, S.; Hamachi, I. *J. Am. Chem. Soc.* **2002**, *124*, 10954–10955.
(18) García, F.; García, J.M.; García-Acosta, B.; Martínez-Máñez, R.; Sancerón, F.; Soto, J. *Chem. Commun.* **2005**, 2790–2792.
(19) Calderón, V.; García, F.; de la Peña, J.L.; Maya, E.; García, J.M. *J. Polym. Sci. Part A: Polym. Chem.* **2006**, *44*, 2270–2281.
(20) Calderón, V.; García, F.; de la Peña, J.L.; Maya, E.; Lozano, A.E.; de la Campa, J.G.; de Abajo, J.; García, J.M. *J. Polym. Sci. Part A: Polym. Chem.* **2006**, *44*, 4063–4075.
(21) Calderón, V.; Shcwarz, G.; García, F.; Tapia, M.J.; Valente, A.J.M.; Burrows, H.D.; de la Peña, J.L.; García, J.M. *J. Polym. Sci. Part A: Polym. Chem.* **2006**, *44*, 6252–6269.
(22) San-José, N.; Gómez-Valdemoro, A.; García, F.C.; Serna, F.; García, J.M. *J. Polym. Sci. Part A: Polym. Chem.* **2007**, *45*, 4026–4036.
(23) San-José, N.; Gómez-Valdemoro, A.; García, F.C.; de la Peña, J.L.; Serna, F.; García, J.M. *J. Polym. Sci. Part A: Polym. Chem.* **2007**, *45*, 5398–5407.
(24) San-Jose, N.; Gómez-Valdemoro, A.; Estevez, P.; García, F.C.; Serna, F.; García, J.M. *Eur. Polym. J.* **2008**, *44*, 3578–3587.
(25) San-José, N.; Gómez-Valdemoro, A.; Calderón, V.; de la Peña, J.L.; Serna, F.; García, F.C.; García, J.M. *Supramol. Chem.* **2009**, *21*, 337–343.
(26) Calderón, V.; Serna, F.; García, F.; de la Peña, J.L.; García, J. *J. Appl. Polym. Sci.* **2007**, *106*, 2875–2884.
(27) Tapia, M.J.; Valente, A.J.M.; Burrows, H.D.; Calderón, V.; García, F.; García, J.M. *Eur. Polym. J.* **2007**, *43*, 3838–3848.
(28) Gómez-Valdemoro, A.; Calderón, V.; San-Jose, N.; García, F.C.; de la Peña, J.L.; Garcia, J.M. *J. Polym. Sci. Part A: Polym. Chem.* **2009**, *47*, 670–681.
(29) San-Jose, N.; Gómez-Valdemoro, A.; García, F.C.; Calderón, V.; García, J.M. *React. Funct. Polym.* **2008**, *68*, 1337–1345.
(30) Rubio, F.; García, F.; Burrows, H.D.; Pais, A.A.C.C.; Valente, A.J.M.; Tapia, M.J.; García, J.M. *J. Polym. Sci. Part A: Polym. Chem.* **2007**, *45*, 1788–1799.
(31) Tapia, M.J.; Burrows, H.D.; García, J.M.; García, F.; Pais, A.A.C.C. *Macromolecules* **2004**, *37*, 856–862.
(32) Tiemblo, P.; Guzmán, J.; Riande, E.; García, F.; García, J.M. *Polymer* **2003**, *44*, 6773–6780.
(33) Trigo-López, M.; Estévez, P.; San-José, N.; Gómez-Valdemoro, A.; García, F.C.; Serna, F.; de la Peña, J.L.; García, J.M. *Recent Patents Aromatic Polyamides* **2009**, *2*, 190–208.
(34) Kutepov, D.F. *Russ. Chem. Rev.* **1962**, *31*, 633–655.
(35) Boerrigter, H.; Grave, L.; Nissink, J.E.M.; Chrisstoffels, L.A.J.; van der Maas, J.H.; Verboom, W.; de Jong, F.; Reinhoudt, D.N. *J. Org. Chem.* **1998**, *63*, 4174–4180.
(36) Kim, S.K.; Yoon, J. *Chem. Commun.* **2002**, 770–771.
(37) Werner, F.; Schneider, H.J. *Helv. Chim. Acta* **2000**, *83*, 465–478.
(38) Sasaki, S.; Citterio, D.; Ozawa, S.; Suzuki, K. *J. Chem. Soc. Perkin Trans. 2* **2001**, 2309–2313.
(39) Xie, H.; Yi, S.; Yang, X.; Wu, S. *New. J. Chem.* **1999**, *23*, 1105–1110.
(40) Mei, M.; Wu, S. *New. J. Chem.* **2001**, *25*, 471–475.
(41) Miyaji, H.; Collinson, S.R.; Prokes, I.; Tucker, J.H.R. *Chem. Commun.* **2003**, 64–65.
(42) Jiménez, S.; Martínez-Máñez, R.; Sancenón, F.; Soto, J. *Tetrahedron Lett.* **2002**, *43*, 2823–2825.
(43) Lee, C.; Lee, D.H.; Hong, J.I. *Tetrahedron Lett.* **2001**, *42*, 8665–8668.
(44) Jose, D.A.; Kumar, D.K.; Ganguly, B.; Das, A. *Tetrahedron Lett.* **2005**, *46*, 5343–5346.
(45) Kim, Y.J.; Kwak, H.; Lee, S.J.; Lee, J.S.; Kwon, H.J.; Nam, S.H.; Lee, K.; Kim, C. *Tetrahedron* **2006**, *62*, 9635–9640.
(46) Jose, D.A.; Dumar, D.K.; Ganguly, B.; Das, A. *Org. Lett.* **2004**, *6*, 3445–3448.
(47) Otón, F.; Tárraga, A.; Espinosa, A.; Velasco, M.V.; Molina, P. *J. Org. Chem.* **2006**, *71*, 4590–4598.
(48) Yang, Y.; Liu, Z.Q.; Zhou, A.G.; Shi, E.X.; Li, F.Y.; Du, Y.K.; Yi, E.; Huang, C.H. *Tetrahedron Lett.* **2006**, *47*, 2911–2914.
(49) Yang, H.; Zhou, Z.G.; Xu, J.; Li, F.Y.; Yi, T.; Huang, C.H. *Tetrahedron* **2007**, *63*, 6732–6736.
(50) Duke, R.M.; Gunnlaugsson, T. *Tetrahedron Lett.* **2007**, *48*, 8043–8047.
(51) Yin, Z.; Liu, S. *Chin. J. Chem.* **2009**, *27*, 43–48.
(52) dos Santos, C.M.G.; McCabe, T.; Watson, G.W.; Kruger, P.E.; Gunnlaugsson, T. *J. Org. Chem.* **2008**, *73*, 9235–9244.
(53) Chauhan, S.M.S.; Bisht, T.; Garg, B. *Tetrahedron Lett.* **2008**, *49*, 6646–6649.
(54) dos Santos, C.M.G.; Gunnlaugsson, T. *Supramol. Chem.* **2009**, *21*, 173–180.
(55) Alajarín, M.; Pastor, A.; Orenes, R.A.; Martínez-Viviente, E.; Rüegger, H.; Pregosin, P.S. *Chem. Eur. J.* **2007**, *13*, 1559–1569.
(56) Alajarín, M.; Pastor, A.; Orenes, R.A.; Steed, J.W. *J. Org. Chem.* **2002**, *67*, 7091–7095.
(57) Alajarín, M.; Pastor, A.; Orenes, R.A.; Steed, J.W.; Arakawa, R. *Chem. Eur. J.* **2004**, *10*, 1383–1397.
(58) Esteban-Gomez, D.; Fabbrizzi, L.; Licchelli, M. *J. Org. Chem.* **2005**, *70*, 5717–5720.
(59) Connors, K. *Binding Constants: The Measurement of Molecular Complex Stability*; Wiley: New York, 1987; Chapter 5.
(60) Al-Soufi, W.; Ramos Cabrer, P.; Jover, A.; Budal, R.M.; Tato, J.V. *Steroids* **2003**, *68*, 43–53.
(61) Cabrer, P.R.; Alvarez-Parrilla, E.; Meijede, F.; Seijas, J.A.; Núñez, E.R.; Tato, J.V. *Langmuir* **1999**, *15*, 5489–5495.

(62) Gil, V.M.S.; Oliveira, N.C. *J. Chem. Edu.* **1990**, *67*, 473−478.
(63) Cabrer, P.R.; Alvarez-Parrilla, E.; Al-Soufi, W.; Meijede, F.; Núñez, E.R.; Tato, J.V. *Supramol. Chem.* **2003**, *15*, 33−43.
(64) Origin 8, OriginLab Corporation, Northampton, MA, USA.
(65) DMSO Reaction Solvent Guide, Technical Bulletin, No. 105B, Gaylord Chemical Corp., Slidell, LA, USA. 2005. (http://www.gaylordchemical.com/bulletins/Bulletin105B/index.htm)
(66) Spartan'08, Wavefunction, Inc., Irvine, CA, USA.
(67) *Matlab 7.8*; MathWorks, Natick, MA, USA.